Capacity of Multiple-Input Multiple-Output Wireless Communication Systems Operating in the HF Band

by

Nigel Leonard Brine

B E (Computer Systems Engineering)

Thesis submitted for the degree of

Doctor of Philosophy

in

School of Electrical and Electronic Engineering,
Faculty of Engineering,
Computer and Mathematical Sciences

The University of Adelaide, Australia

2010

Chapter 7

Correlation Calculations

Recall that in Chapter 5 an alternate approach to calculating HF MIMO capacity was devised which involves using the Gesbert MIMO channel matrix model equation (5.2) to generate channel matrices from antenna correlation and mode correlation matrices. The generated channel matrices are substituted into the general MIMO capacity equation with no CSI (2.9) to produce capacity results. The MCR was developed in order to record HF radio data from which antenna and mode correlation matrices can be generated. In this chapter the techniques devised for generating the antenna and mode correlation matrices from the recorded HF radio data are described, along with a technique devised for calculating time correlation.

In Chapter 6 it was shown that the recorded HF radio data can be processed to generate ionograms which reveal the propagating modes present at each frequency of the HF band. The mode peaks at a given frequency can be detected using the approach described in Section 6.5. Signals for each detected mode can be generated by applying a phase shift, which is a function of the frequency and group delay of the mode, to a base signal at the frequency of interest, using Equations (6.1)–(6.5) from Section 6.2. Correlation matrices can be generated from these signals. Correlation between two complex signals X and Y is given by [83]

$$\rho_{env} = \left| \frac{E\{(X - E\{X\})(Y - E\{Y\})^*\}}{\sqrt{E\{|X - E\{X\}|^2\} E\{|Y - E\{Y\}|^2\}}} \right| \tag{7.1}$$

where $*$ is the complex conjugate, $E\{\cdot\}$ is the expectation operator, and $|\cdot|$ is the complex magnitude operator. This is the general approach taken in order to perform antenna, mode and

time correlation calculations. The specific techniques devised for the antenna, mode and time correlation calculations are described in the following sections.

7.1 Calculating Antenna Correlation from Ionograms

To calculate antenna correlation, the signal paths shown in Figure 7.1 are considered. The steps for calculating antenna correlation are outlined in Figure 7.2. For each antenna, the group delay FFT at block index i_b of an ionogram is processed to detect the mode peaks. Mode peaks not seen on all antennas are identified by comparing FFT indexes, and removed, leading to conservative correlation calculations. Signals for each propagating mode and antenna combination are generated by applying a phase shift, which is a function of frequency (and hence block index i_b) and group delay of the mode, to a base signal with frequency corresponding to block index i_b. An overall signal sample is obtained for each antenna by summing the signals for each propagating mode, and letting $t = 0$. The overall signal samples for each antenna at block index i_b of each recorded ionogram form the set of samples used for the antenna correlation calculations. Antenna correlation matrices are generated for each block index i_b, which can be used to calculate an average antenna correlation matrix, and to generate antenna correlation versus frequency plots. Note that only overall signal samples featuring three or more modes were considered in calculating antenna correlation, in order to represent a situation where significant multipath is present.

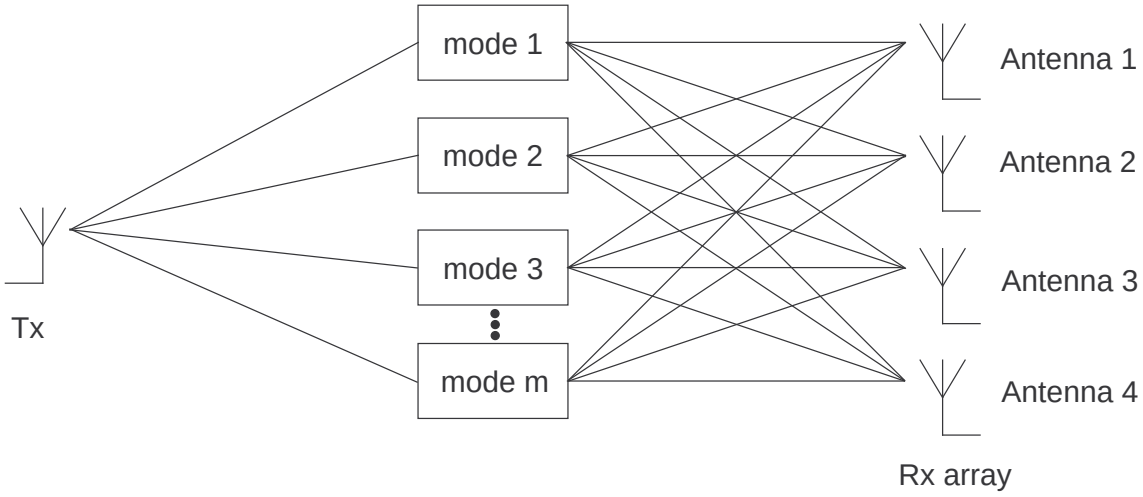

Figure 7.1. Signal paths for the antenna correlation calculations

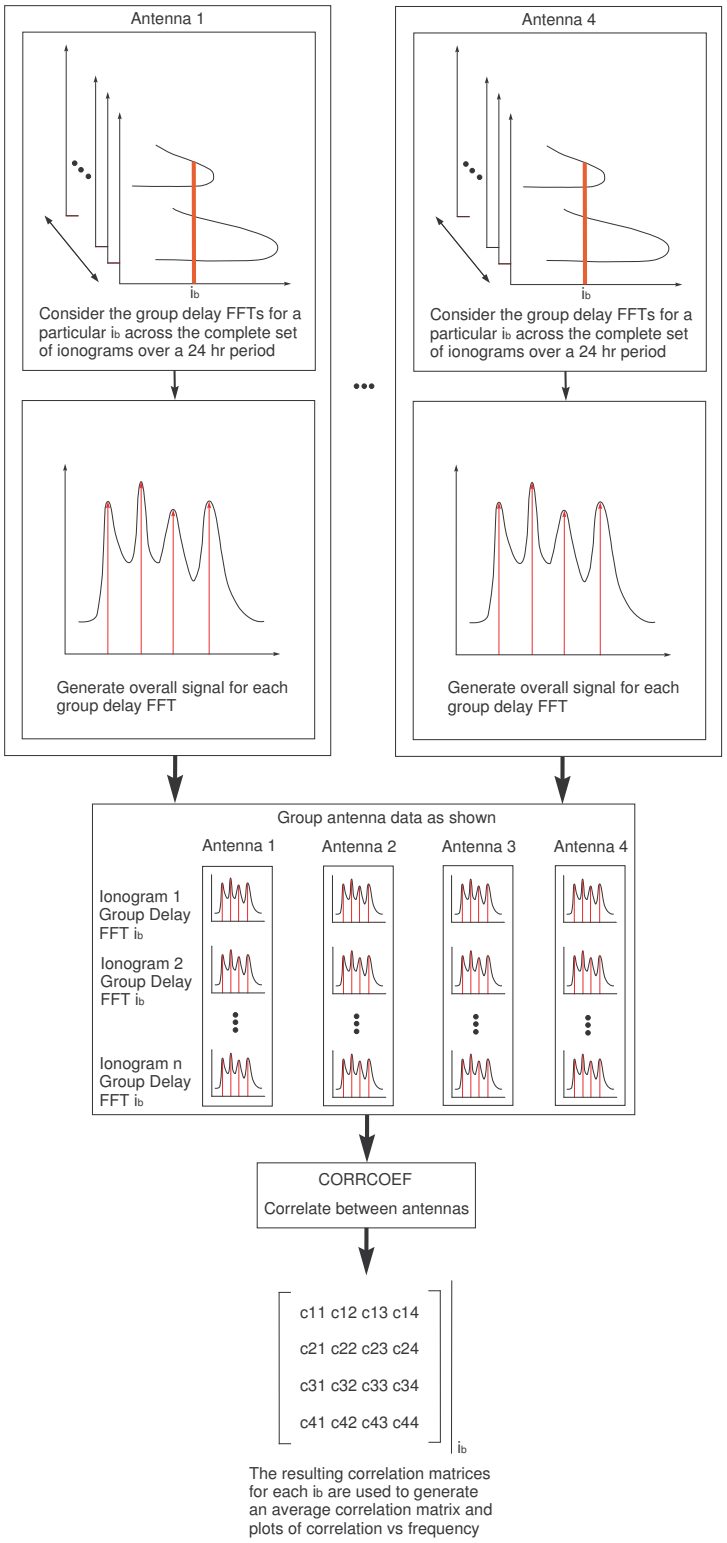

Figure 7.2. A diagram outlining the steps required for calculating antenna correlation

7.1.1 Antenna Correlation Results

Antenna correlation calculations were performed on 65 ionograms recorded over a 24 hour period using the receive antenna array shown in Figure 6.2. As discussed in Section 6.3, in order to generate signals of accurate phase for correlation calculations we require $\Delta_{d_\lambda} << \lambda$. N_{FFT} was set to 2^{20}, corresponding to a Δ_{d_λ} of $0.17\ \lambda$ at 25 MHz.

The number of samples used to calculate antenna correlation at each frequency is shown in Figure 7.3, while the plot of antenna correlation versus frequency for antennas 1 and 2 is shown in Figure 7.4. Table 7.1 shows the average antenna correlation matrix, which was obtained by averaging correlation between pairs of antennas across the entire range of frequencies. Average antenna correlation across the HF band of frequencies was found to be around 0.53, however correlation was found to fluctuate considerably, as can be seen in Figure 7.4. Correlation between antennas 3 and 4, which are 13.5 m apart, did not seem to be any higher than correlation between the other pairs of antennas, which are spaced further apart. The antenna correlation calculations should be repeated with a linear array of antennas to investigate how correlation varies with antenna separation, and establish the minimum antenna separation necessary for adequate decorrelation.

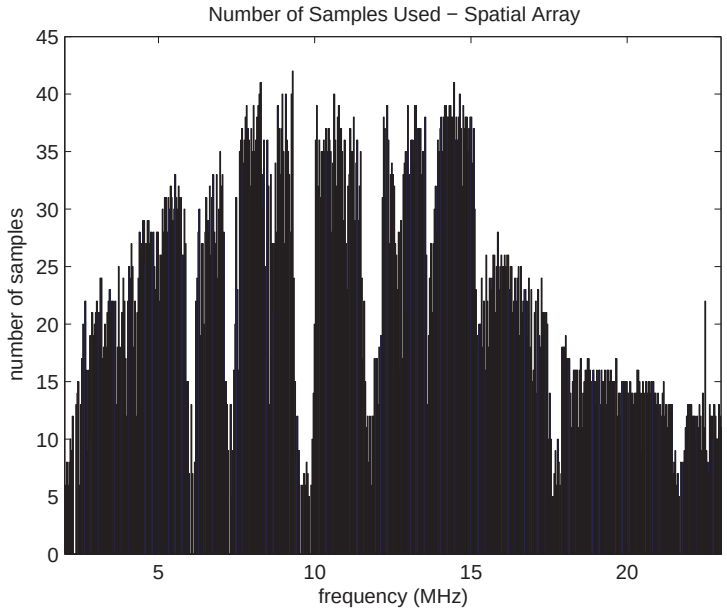

Figure 7.3. Number of samples versus frequency

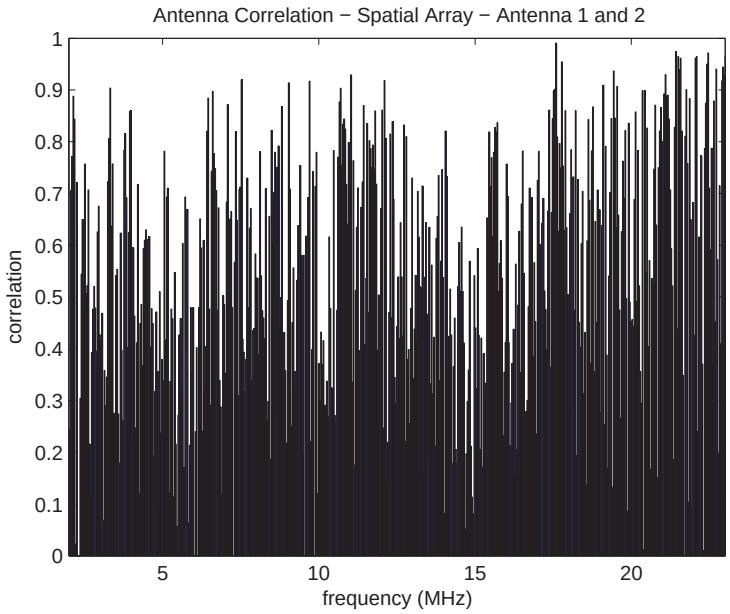

Figure 7.4. Antenna correlation versus frequency - antenna 1 and 2

Average Correlation Matrix	Antenna Index i			
Antenna Index j	1	2	3	4
1	1.0000	0.5450	0.5293	0.5347
2	0.5450	1.0000	0.5185	0.5365
3	0.5293	0.5185	1.0000	0.5301
4	0.5347	0.5365	0.5301	1.0000

Table 7.1. Average antenna correlation matrix

7.2 Calculating Mode Correlation from Ionograms

To calculate mode correlation, the signal paths shown in Figure 7.5 are considered. The steps for calculating mode correlation are outlined in Figure 7.6. HF radio data recorded for a single receive antenna is used. Because modes change in time and frequency, the data is processed using a very large block overlap in order to increase time resolution. A set of consecutive overlapping blocks are considered for each mode correlation calculation, and several blocks between each set of considered blocks are discarded to reduce the amount of processing required for each ionogram. The number of consecutive blocks used for each calculation is kept relatively small, so that change in frequency is small across the set. For a set of consecutive blocks, the group delay FFTs are processed to obtain the mode peaks. Data from an additional antenna is used to help avoid detecting a large noise fluctuation as a mode peak. Mode peaks not detected for all of the group delay FFTs are identified by comparing FFT indexes, and removed. A signal sample for each mode is generated by applying a phase shift, which is a function of frequency (and hence block index) and group delay of the mode, to a base signal at the frequency corresponding to the block index. The signal samples for each of the identified modes across the consecutive blocks form the set of samples used for the mode correlation calculations.

Mode correlation calculations used to generate the capacity results presented in Chapter 8 were performed using $N_{FFT} = 2^{20}$, a block size of 512 samples and a block overlap of 507 samples, while 10 consecutive blocks of data were used for each calculation. By reducing the sweep rate of the ionosonde transmit signal, or by using a narrowband sawtooth sweep signal tuned to a frequency of interest, a larger number of consecutive blocks of data could be used, resulting in improved mode correlation calculations. These techniques are described further in Chapter 9.

It is important to note that mode correlation calculations vary according to the receive antenna selected, due to the path length variations between antennas. An average mode correlation could be calculated from mode correlation calculations performed for each receive antenna, at the cost of increased processing. This was not done due to the considerable amount of processing already required.

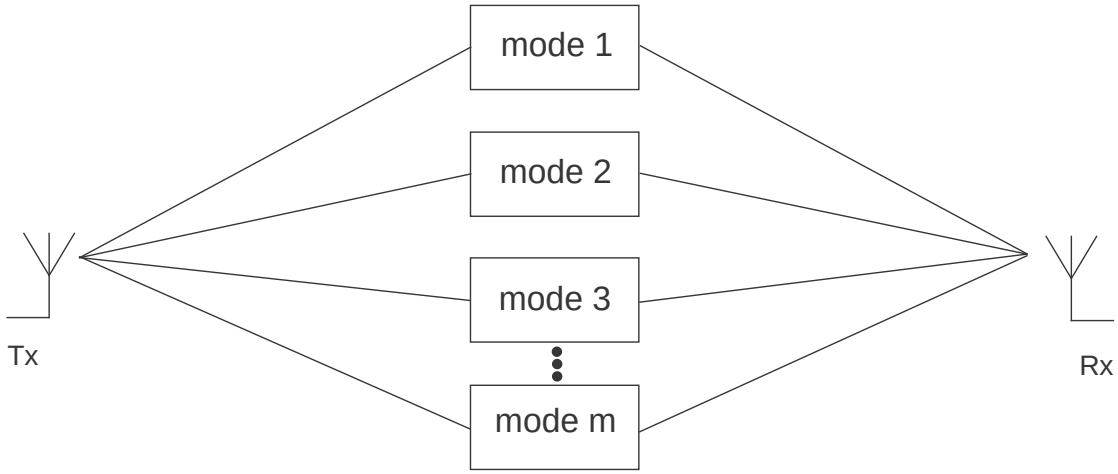

Figure 7.5. Signal paths for the mode correlation calculations

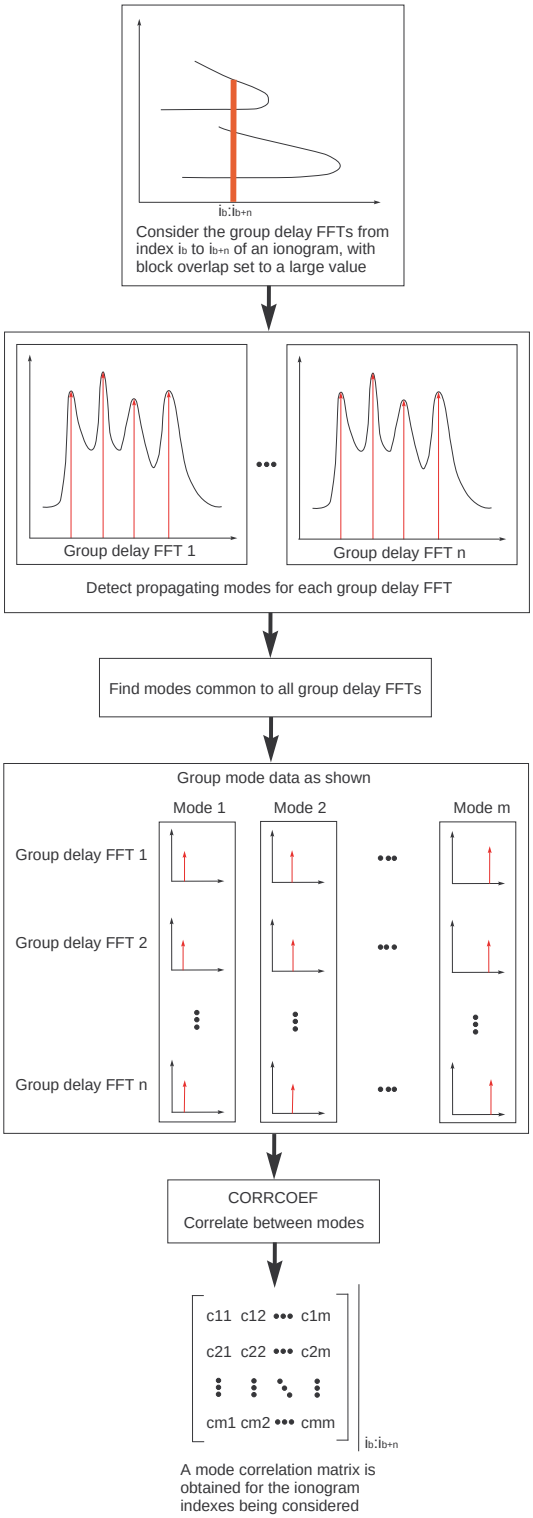

Figure 7.6. A diagram outlining the steps required for calculating mode correlation

7.3 Calculating Time Correlation from Ionograms

The steps for calculating time correlation are outlined in Figure 7.7. HF radio data recorded for a single receive antenna is considered. The transmitter is used to transmit two FMCW signals of equal sweep rate simultaneously, with one signal slightly ahead in frequency over the other. It is important that the two signals originate from exactly the same spatial location to eliminate the effect of spatial decorrelation. The two separate receiver sections of the MCR are used to simultaneously tune to the two sets of receive signals corresponding to the two transmit signals. For each receiver section, the group delay FFT at block index i_b of an ionogram is processed to detect the mode peaks. The block index i_b of the second receiver section is scaled so that it points to the same frequency as the i_b of the first receiver section. This is important since we wish to compare the state of the channel at exactly the same frequency, but at a slightly different time. Mode peaks not seen by each receiver section are identified by comparing FFT indexes, and removed. Signals for each propagating mode and receiver section combination are generated by applying a phase shift, which is a function of frequency (and hence block index i_b) and group delay of the mode, to a base signal at the frequency corresponding to the block index i_b. An overall signal sample is obtained for each receiver section by summing the signals for each propagating mode, and letting $t = 0$. The overall signal samples for each receiver section at block index i_b of each recorded ionogram form the set of samples used for the time correlation calculations. Time correlation matrices are generated for each i_b, which can be used to calculate an average time correlation matrix, and to generate time correlation versus frequency plots.

While it is preferable for antennas and modes to be highly decorrelated, such that channel matrix rank is large, it is preferable for time correlation to be high. The slower the state of the channel changes, the longer a channel matrix estimate remains valid. Channel matrix estimates are typically made at the receive end of MIMO systems, and used in the spatial processing algorithm to recover the transmit signal vector. A fast changing channel means that the interval between channel matrix estimates needs to be short. If the channel changes very quickly, then unitary space-time modulation should be used [70].

By varying the frequency difference between the two transmit signals, and repeating the time correlation calculation process described, the time correlation for different time intervals can be investigated, and an appropriate interval between channel matrix estimates determined. However, no transmitter with the ability to transmit two FMCW signals simultaneously from the same spatial location was available, so time correlation calculations could not be performed.

Figures 7.8, 7.9, 7.10 and 7.11 show examples of pairs of ionograms recorded 2, 4, 6 and 8 seconds apart. While the transmit antennas were reportedly located on the same site, each pair of ionograms are uncorrelated, indicating that transmit antenna separation was very large. The transmit antennas need to be co-located for time correlation calculations to be performed.

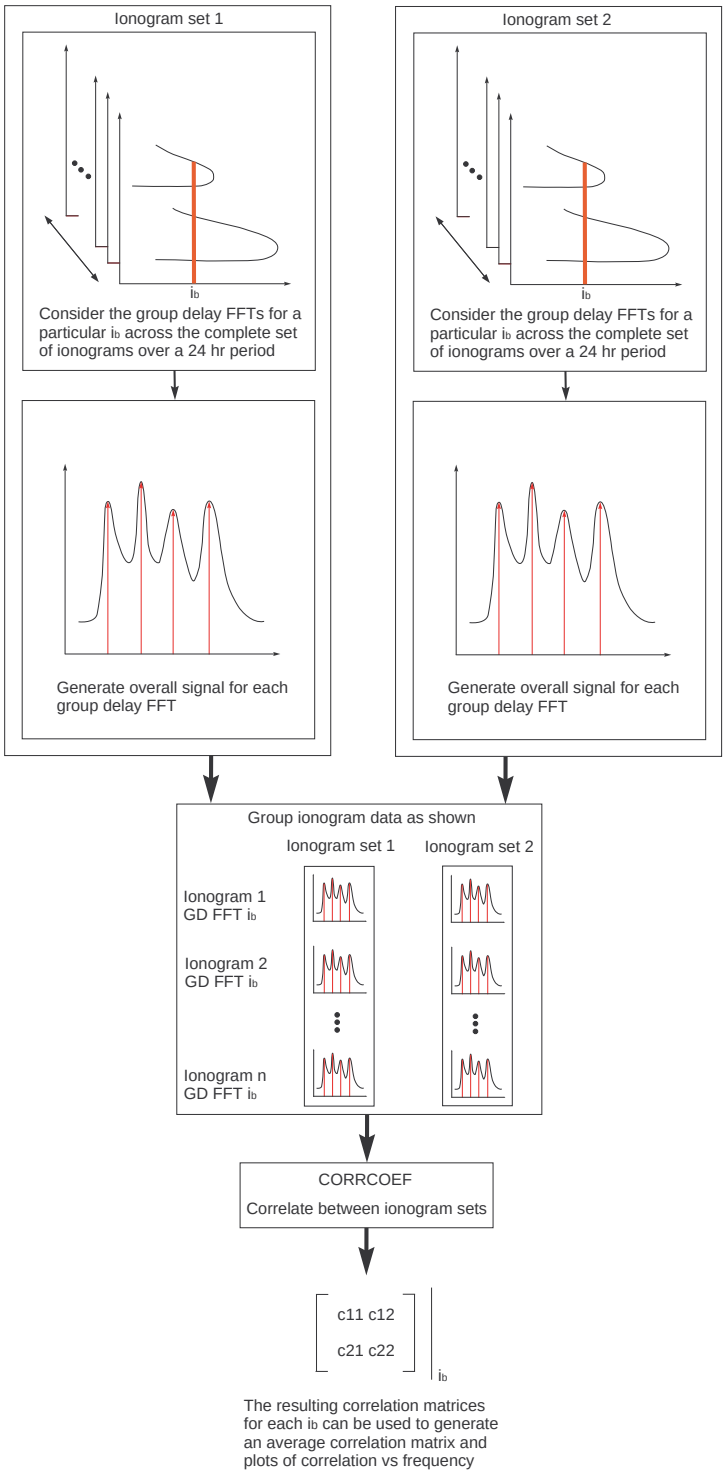

Figure 7.7. A diagram outlining the steps required for calculating time correlation

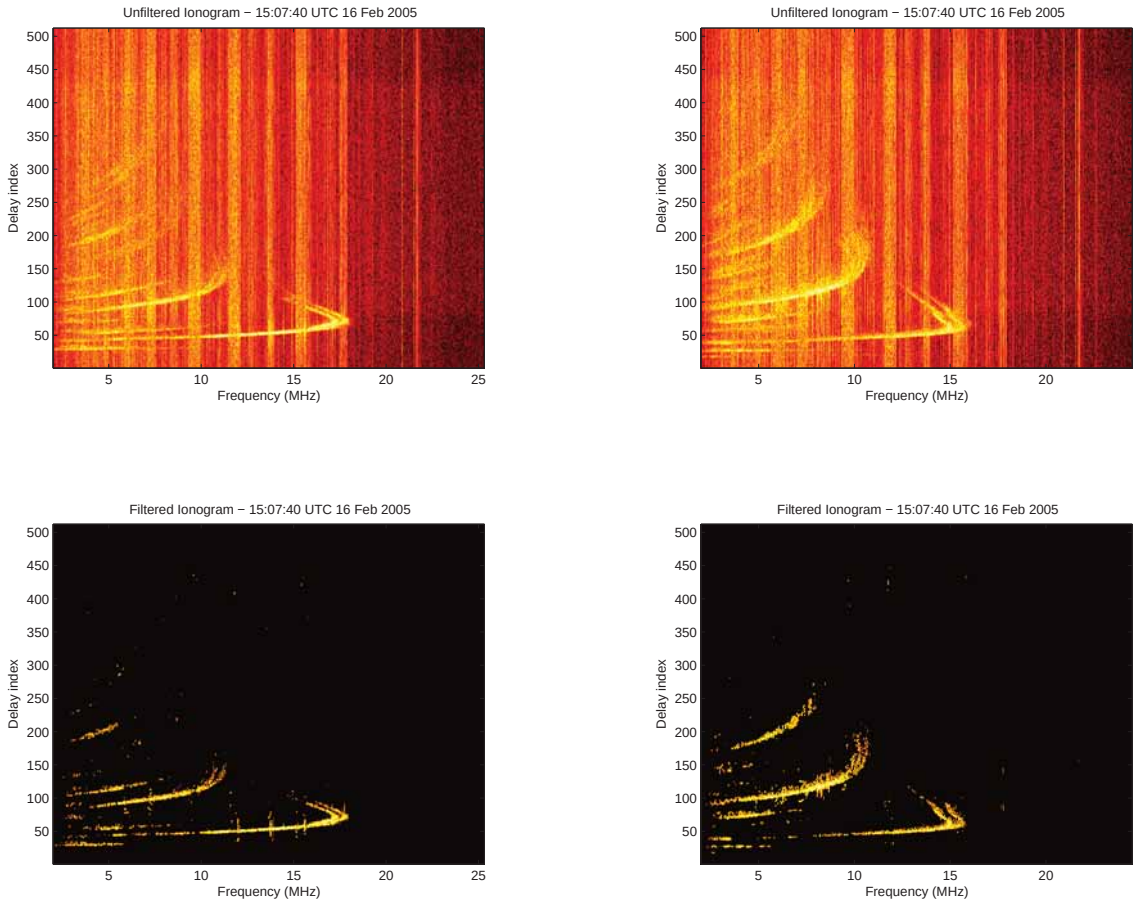

Figure 7.8. Ionograms recorded two seconds apart

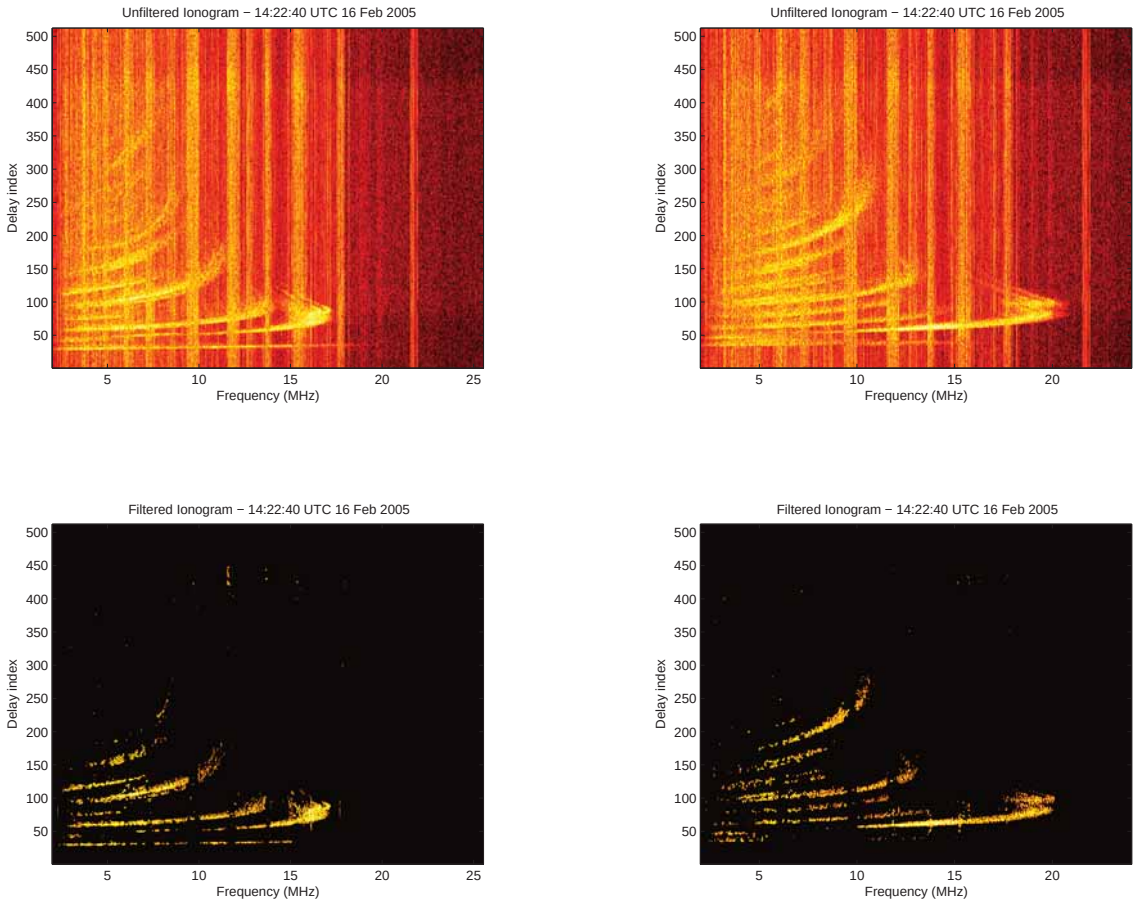

Figure 7.9. Ionograms recorded four seconds apart

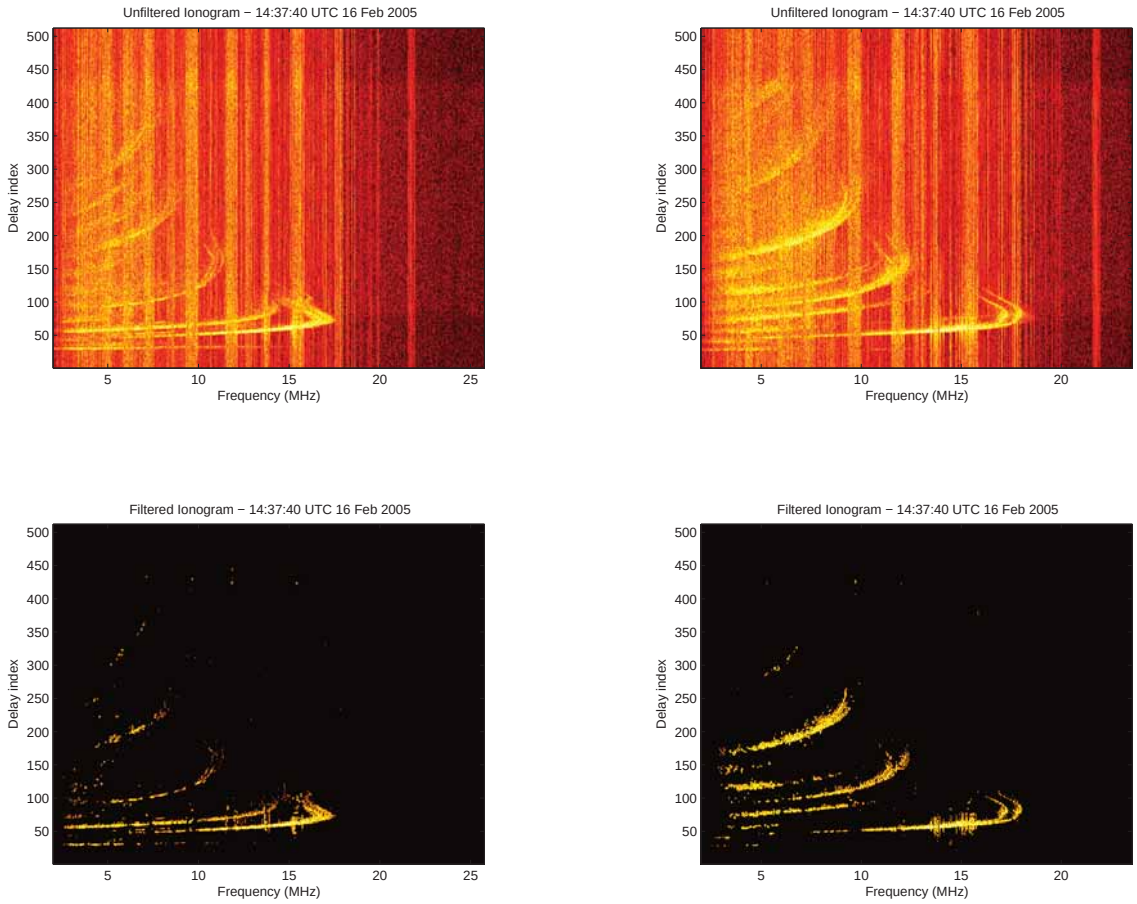

Figure 7.10. Ionograms recorded six seconds apart

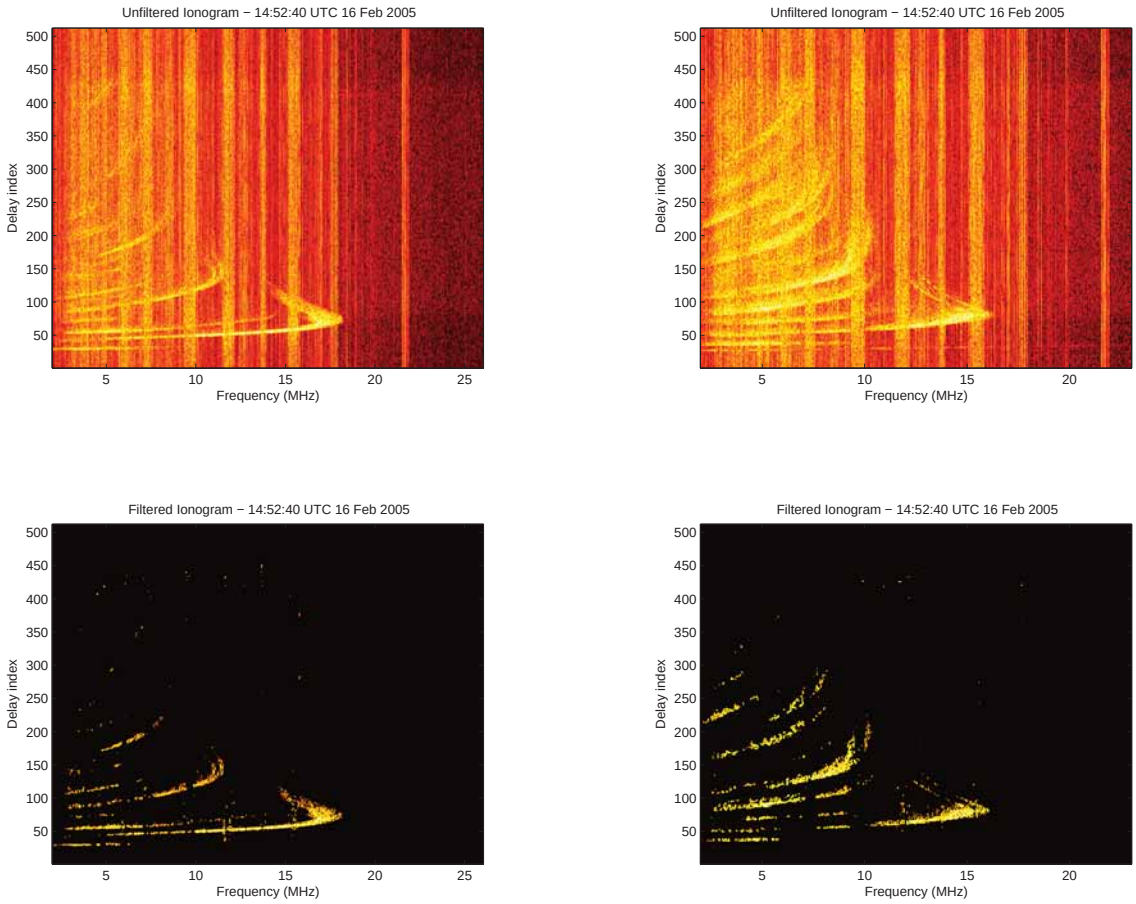

Figure 7.11. Ionograms recorded eight seconds apart

7.4 Summary

In this chapter, techniques devised for calculating antenna, mode and time correlation from recorded HF radio data were described. Antenna and mode correlation calculations were performed using these techniques, however time correlation calculations could not be performed, since no transmitter with the ability to transmit two FMCW signals simultaneously from the same spatial location was available. Average antenna correlation across the HF band of frequencies was found to be around 0.53. The antenna correlation calculations should be repeated for a linear array of antennas to investigate how correlation varies with antenna separation, and establish the minimum antenna separation necessary for adequate decorrelation. Mode correlation calculations were performed using 10 consecutive blocks of data at a time. By reducing the sweep rate of the ionosonde transmit signal, or by using a narrowband sawtooth sweep signal tuned to a frequency of interest, a larger number of consecutive blocks of data could be used, resulting in improved mode correlation calculations. Antenna and mode correlation matrices were substituted into the Gesbert MIMO channel matrix model equation (5.2) in order to generate channel matrices for HF MIMO capacity calculations. Details of the HF MIMO capacity calculations are provided in the next chapter.

This page is blank

Chapter 8

HF MIMO Capacity Calculations

Having processed the HF radio data in order to determine the number of modes present, and to generate antenna and mode correlation matrices, HF MIMO capacity calculations can now be performed. Recall from Chapter 5 that the Gesbert channel model generates a channel matrix according to the equation

$$\boldsymbol{H} = \frac{1}{\sqrt{m}}(\boldsymbol{C}_r)^{\frac{1}{2}}\boldsymbol{G}_{rm}(\boldsymbol{C}_m)^{\frac{1}{2}}\boldsymbol{G}_{mt}(\boldsymbol{C}_t)^{\frac{1}{2}}.$$

The matrices $\boldsymbol{G}_{mt}$ and $\boldsymbol{G}_{rm}$ contain Rayleigh distributed entries, while the antenna correlation matrices $\boldsymbol{C}_t$ and $\boldsymbol{C}_r$, and mode correlation matrices $\boldsymbol{C}_m$ can either be set to identity matrices of size $m \times m$, where m is the number of modes detected at the time and frequency instant being considered, or to antenna and mode correlation matrices generated using the approaches described in Chapter 7.

The channel matrix $\boldsymbol{H}$ is subsituted into the general MIMO capacity equation to yield capacity. The general MIMO capacity equation with no CSI was stated in Section 2.2.1 as being

$$C = E_H\{\log_2[\det(\frac{P_T}{n_T\sigma_n^2}\boldsymbol{H}\boldsymbol{H}^* + \boldsymbol{I}_{n_R})]\}.$$

HF MIMO capacity calculations were performed with the SNR term $P_T/(n_T\sigma_n^2)$ set to the average of the receive SNR for each propagating mode present, and then adjusted to represent the SNR for a standard HF modem transmit power of 100 W. SNR was measured in a 1.69 Hz bandwidth using the technique described in Section 6.7.2.

With $\boldsymbol{C}_t$, $\boldsymbol{C}_r$ and $\boldsymbol{C}_m$ all set to identity matrices of size m, calculated capacities represent the ideal situation where no antenna or mode correlation is present. With $\boldsymbol{C}_t$ and $\boldsymbol{C}_r$ set to identity matrices, and $\boldsymbol{C}_m$ generated using the mode correlation calculation technique described in Chapter 7, calculated capacities represent the underlying channel capacity, which is dependent on the number of modes and mode correlation. This is because antenna spacing can be increased in order to reduce antenna correlation, however mode correlation cannot be changed.

The results of the HF MIMO capacity calculations are presented in the next section.

8.1 HF MIMO Capacity Results

8.1.1 Capacity for an Example Ionogram

Capacity results for a single example ionogram are first presented. Consider the ionogram recorded at 06:30 UTC (co-ordinated universal time) (17:00 Adelaide time) on 16/02/05, which is shown in Figure 8.1. Capacity for this ionogram was first calculated under the assumption that propagating modes and antennas are fully uncorrelated, by setting mode and antenna correlation matrices to identity matrices of size $m \times m$, where m is the number of detected propagating modes. A plot of the number of detected propagating modes versus frequency is shown in Figure 8.2. Average capacity at each frequency index of the ionogram was calculated by repeating capacity calculations for different $\boldsymbol{G}_{mt}$ and $\boldsymbol{G}_{rm}$ realizations. The plot of average capacity versus frequency obtained under the assumption that propagating modes and antennas are fully uncorrelated is provided in Figure 8.3.

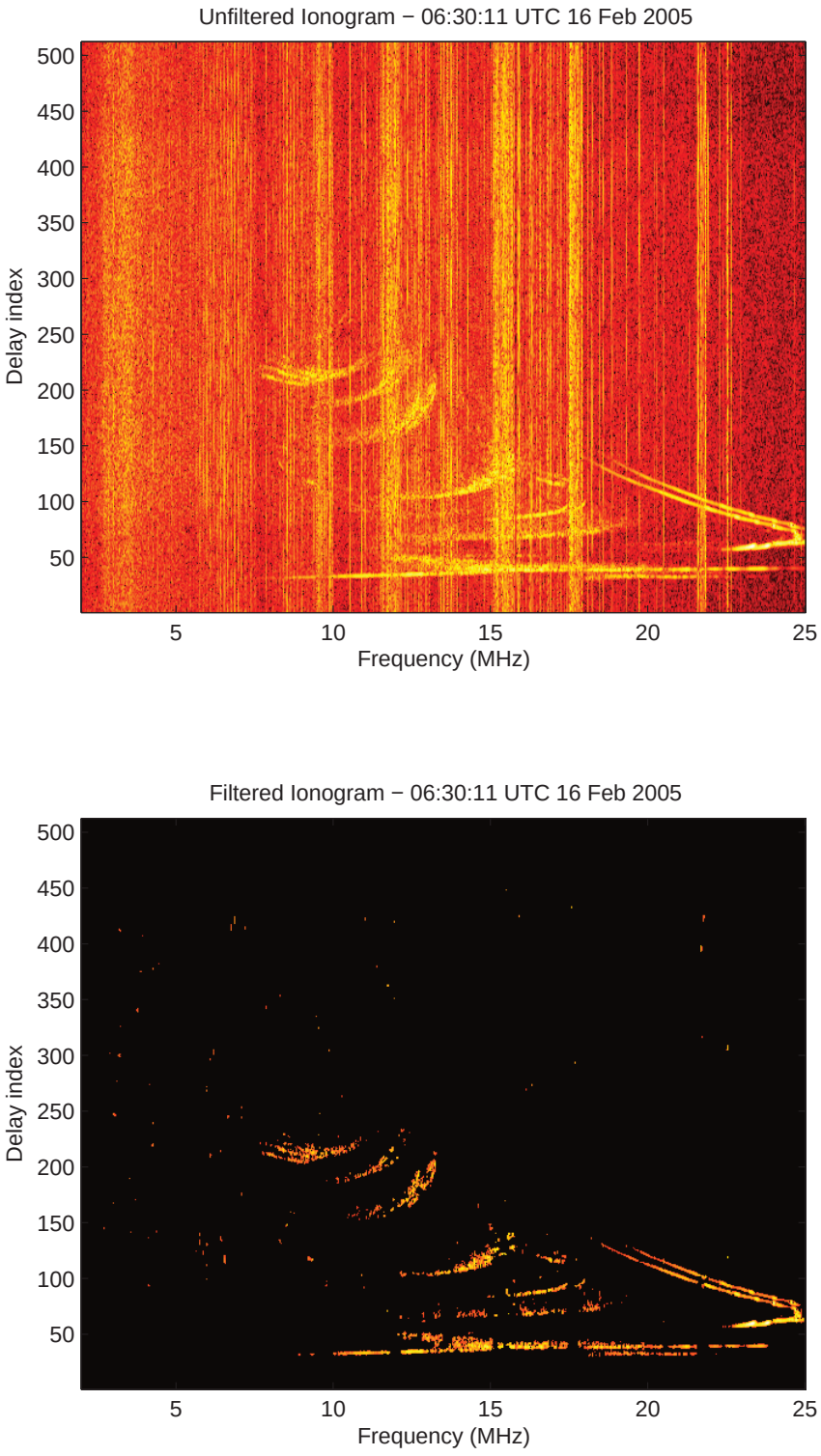

Figure 8.1. The example ionogram being examined

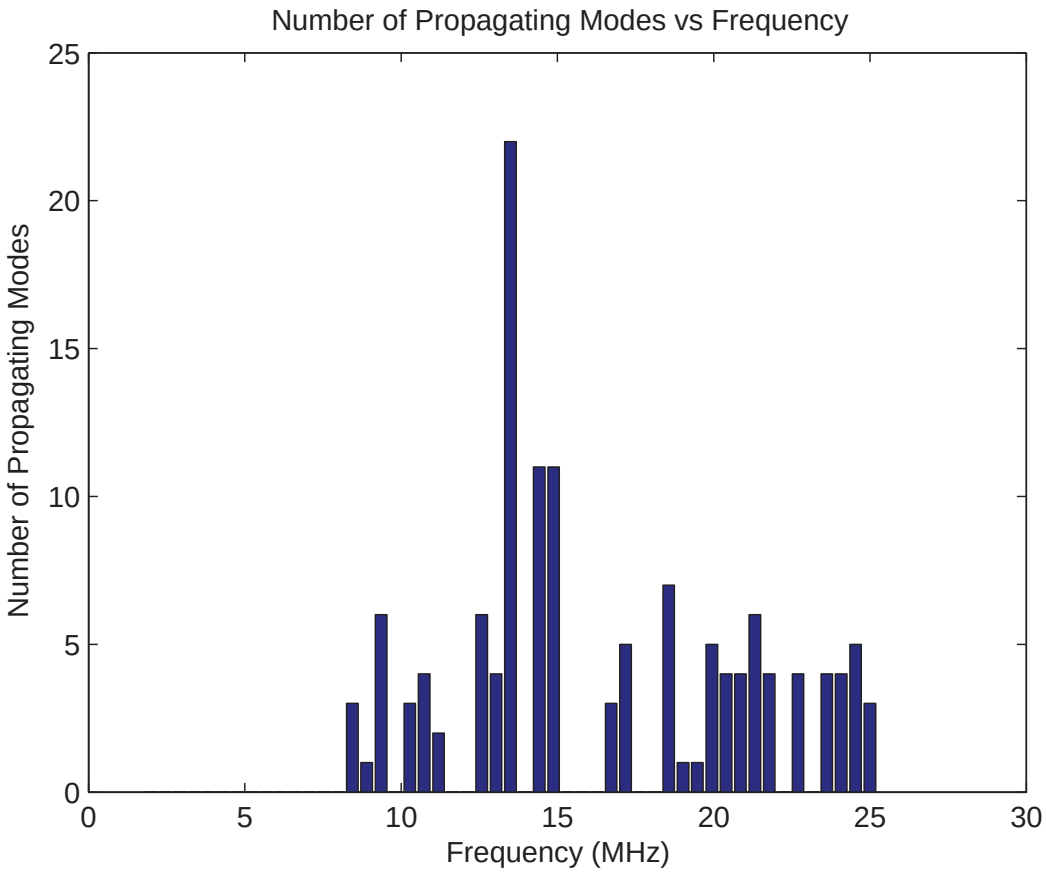

Figure 8.2. Number of propagating modes versus frequency for the example ionogram

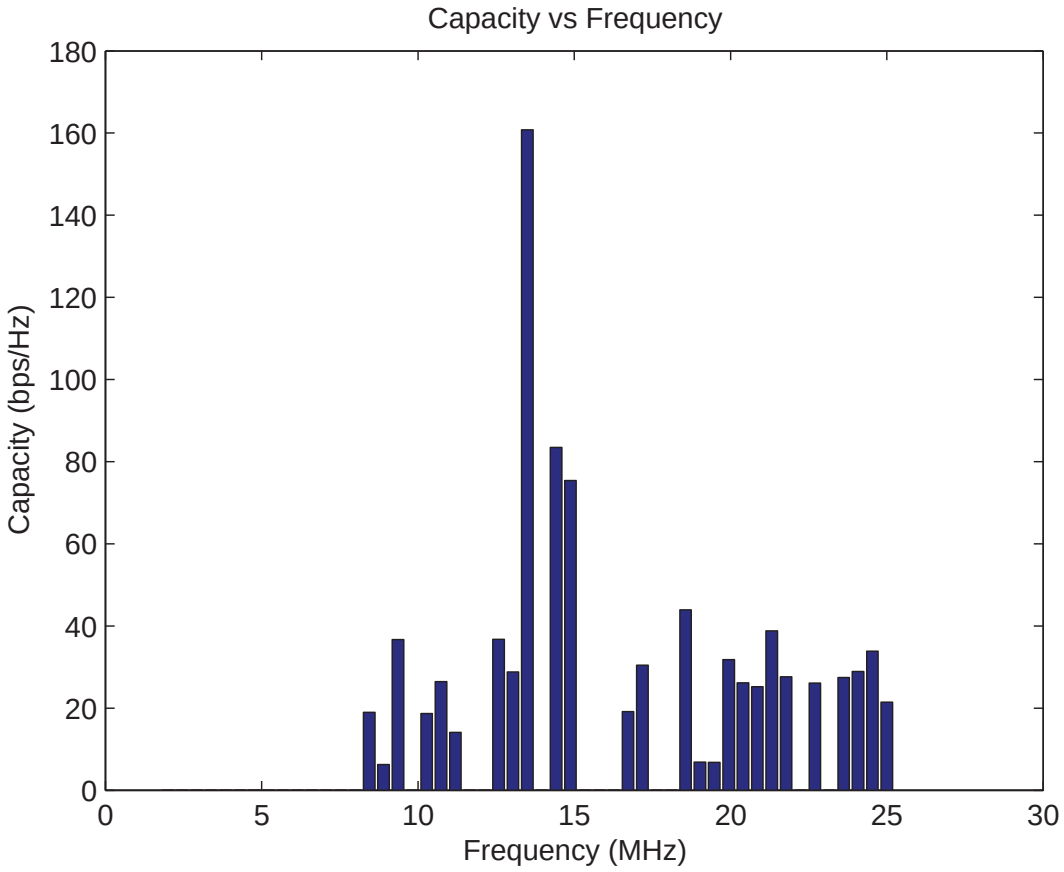

Figure 8.3. Capacity versus frequency for the example ionogram, under the assumption that propagating modes and antennas are fully uncorrelated

Capacity was recalculated with mode correlation matrices obtained using the technique described in Section 7.2, while leaving antenna correlation matrices set to identity matrices of size $m \times m$, so that the underlying capacity of the channel could be investigated. A plot of average channel matrix rank versus frequency was generated, which is shown in Figure 8.4, along with a plot of average capacity versus frequency which is shown in Figure 8.5. Note the similarity between the two plots, due to the linear relationship between channel matrix rank and capacity which was seen in Section 2.2.4.

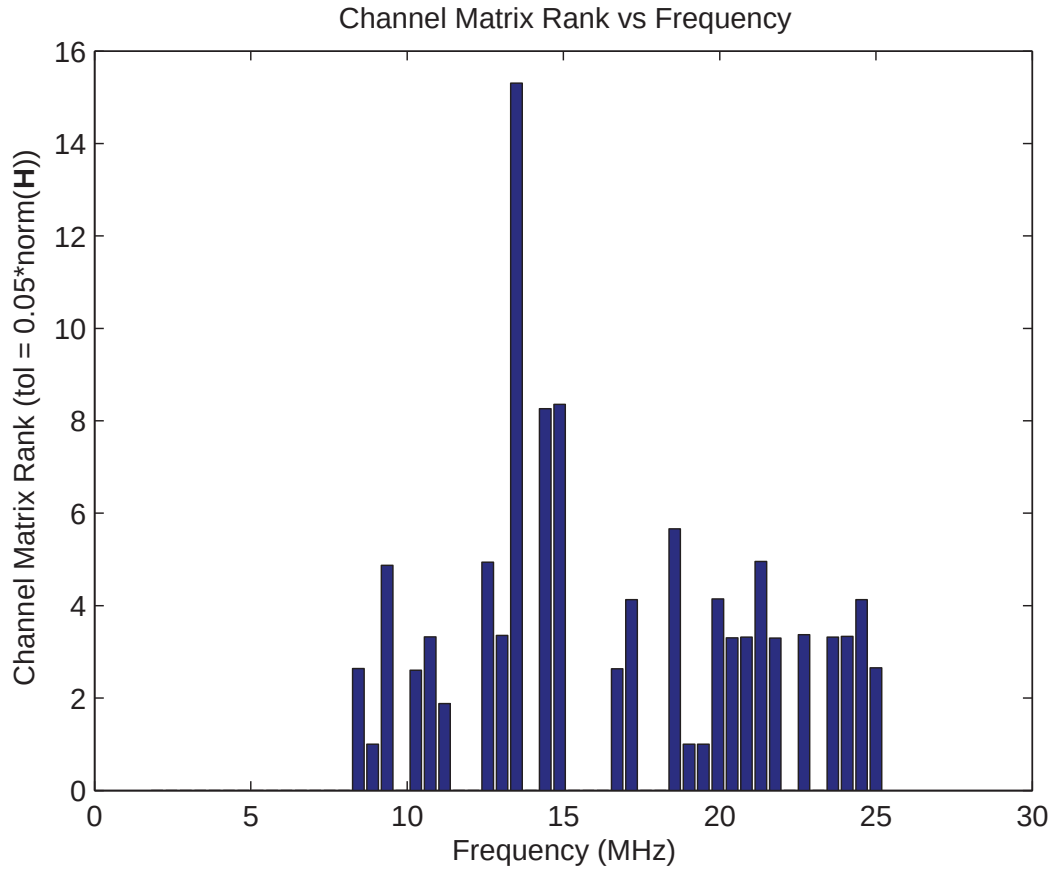

Figure 8.4. Channel matrix rank versus frequency for the example ionogram

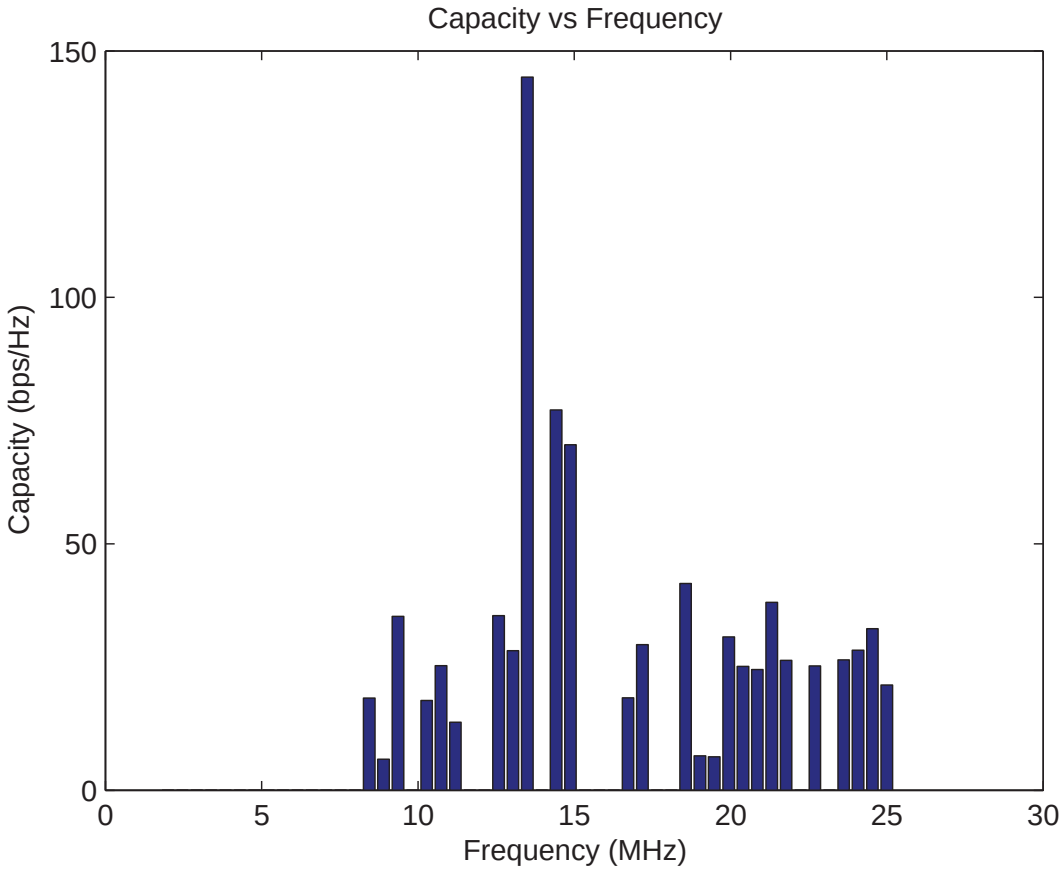

Figure 8.5. Capacity versus frequency for the example ionogram, taking into account mode correlation under the assumption antennas are fully uncorrelated

The frequency index yielding the highest capacity for the example ionogram is 26, which corresponds to a frequency of approximately 13.5 MHz. At this frequency 22 propagating modes are present, and the average channel matrix rank r for a threshold $tol = 0.05$ norm($\boldsymbol{H}$) is approximately 15 when mode correlation is taken into account, where norm is the matrix norm function which calculates the largest singular value of a matrix. This means that for each channel matrix generated by the Gesbert channel matrix model there are on average 15 singular values within 5% of the size of the largest singular value. Average capacity was 161 bps/Hz for the case where mode and antenna correlation matrices were set to identity matrices of size 22×22, and this fell to 145 bps/Hz, when propagating mode correlation was taken into account. Because channel matrix rank is approximately 15, setting antenna correlation matrices to identity matrices of size 15×15 will capture most of the capacity calculated using antenna correlation matrices of size 22×22, and performing this step resulted in an average capacity of 117 bps/Hz. The drop in capacity can be attributed to reduced receive antenna array gain associated with the reduction of n_R and n_T from 22 to 15, and also to the fact rank measurement is an approximation based on a threshold of $tol = 0.05$ norm($\boldsymbol{H}$).

The capacity at 13.5 MHz was recalculated with antenna correlation taken into account by using transmit and receive antenna correlation matrices of size 22×22 constructed to represent the average antenna correlation of 0.53 calculated in Section 7.1.1, such that each matrix element is 0.53, except for the 1s along the main diagonal. Note that while it has been assumed that each pair of antenna elements has the same average correlation, generally each pair of antenna elements will have a different correlation which is dependent on the separation between the elements. Using the mode correlation matrix calculated for frequency index 26, along with the constructed antenna correlation matrices, an average capacity of 114 bps/Hz was obtained. Average channel matrix rank was found to be 11. In order to increase channel matrix rank back up to 15, either antenna correlation needs to be reduced by increasing antenna element separation, or a larger number of antennas needs to be used.

The group delay FFT at 13.5 MHz is shown in Figures 8.6 and 8.7. The path length variation for each of the modes across the 10 mode data samples used to generate the mode correlation matrix is shown in Figure 8.8, and this plot reveals possible problems. The path length for each mode was found to vary by up to 147 wavelengths over the period of 10 samples. Because f_s = 868 S/s, k = 125 kHz/s and $b - \Delta = 5$, 10 samples in this plot corresponds to a period of 57.6 ms and an ionosonde transmit signal frequency increase of 7.2 kHz. The shift in path length is partly due to a change in time, and partly due to a shift in frequency, however the

amount that is due to time, and the amount that is due to frequency, is not known. For the case that the change is entirely due to the change in time, the mode correlation calculations are accurate, and the path length variations encountered indicate that the channel matrix estimate needs to be updated very frequently, or unitary space-time modulation should be used [70]. For the case that the change is entirely due to the change in frequency, the mode correlation calculations are corrupted by the change in frequency, and nothing can be said about an appropriate interval between channel matrix estimates. In order to resolve this issue, mode correlation calculations should be repeated for data collected using a repeating narrowband sweep transmit signal, as described in Chapter 9.

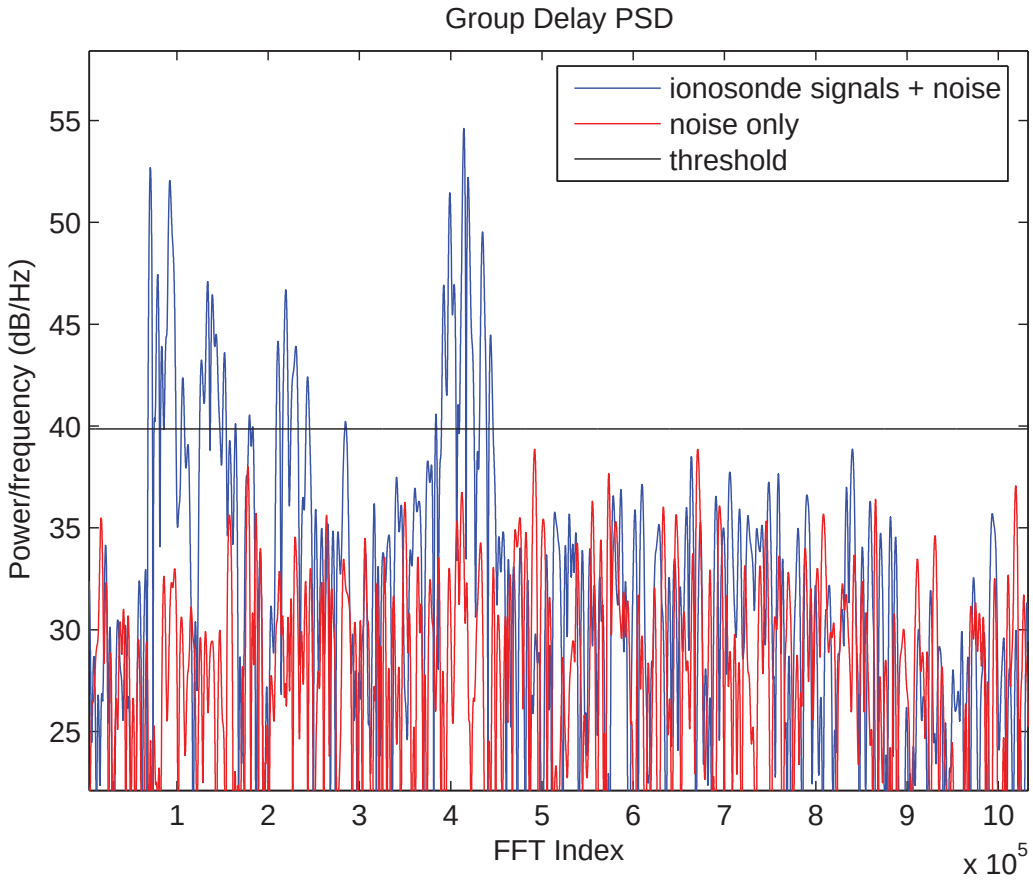

Figure 8.6. The zoomed out view of the group delay FFT at the ionogram frequency index yielding the highest capacity

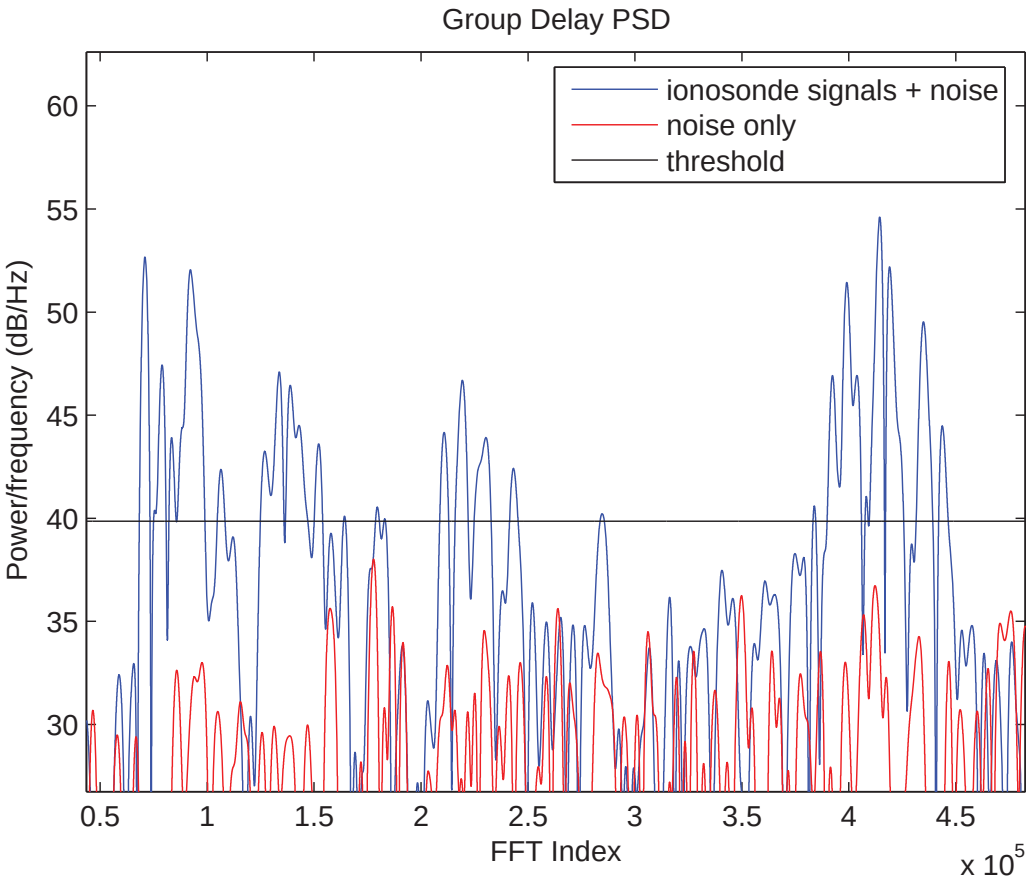

Figure 8.7. The zoomed in view of the group delay FFT at the ionogram frequency index yielding the highest capacity

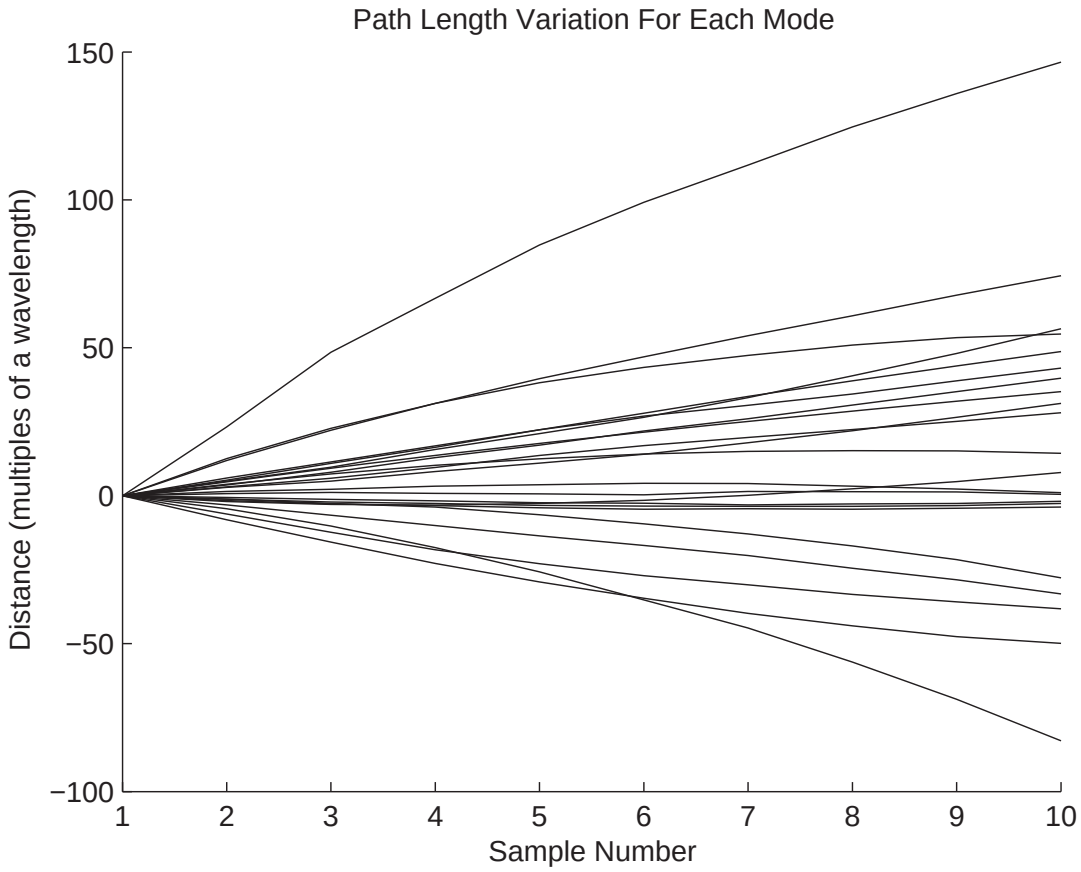

Figure 8.8. The path length variation for each mode across the 10 samples used at the ionogram frequency index yielding the highest capacity

The frequency yielding the highest capacity, 13.5 MHz, corresponds to a focusing point on the ionogram where high and low altitude rays meet. The path length variation was plotted for a more stable frequency of 20 MHz, with the plot shown in Figure 8.9. The path length for each mode in this case was found to vary by up to 50 wavelengths over the period of 10 samples, which is still very high.

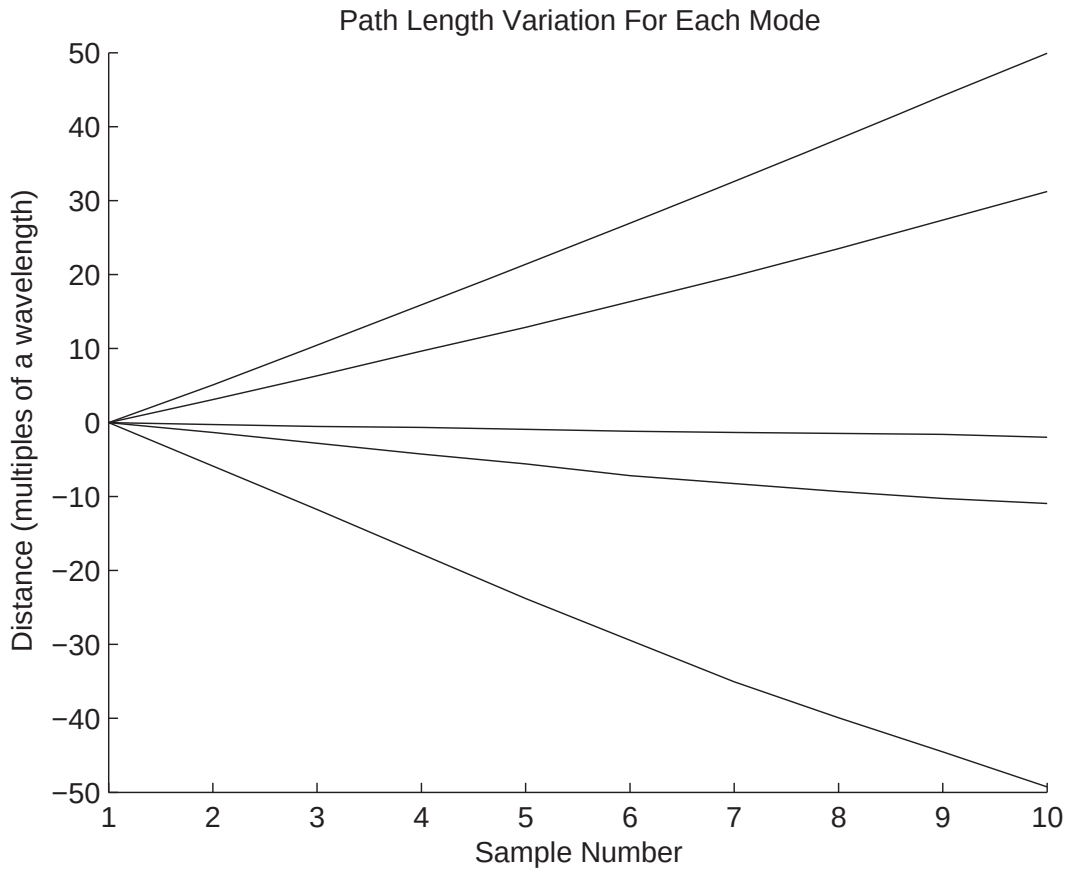

Figure 8.9. The path length variation for each mode across the 10 samples used at 20 MHz

Additional useful calculations include capacity for the case where the propagating modes are fully correlated, and capacity when $n_T = m = n_R = 1$. When propagating modes are fully correlated, capacity is dependent on receive antenna array gain. The mode correlation matrix was set to the all ones matrix to collapse channel matrix rank to 1, while the number of transmit and receive antennas was set to 22. An average capacity of 14 bps/Hz was calculated. Setting $n_T = m = n_R = 1$ yielded an average capacity of 9 bps/Hz, which represents the capacity of a single channel HF system in the absence of multipath.

The Clover 2000 waveform used in HF modems is designed to operate at a spectral efficiency of 0.25 bps/Hz [76] which is considerably lower than the MIMO capacities calculated here. Note however that the Clover-2000 waveform employs 8 tones in a bandwidth of 2 MHz, so a direct comparison between the MIMO capacities calculated here for the narrow bandwidth of 1.69 Hz, and Clover-2000 spectral efficiency, cannot be made.

8.1.2 Capacity Across a Set of Ionograms

The next set of capacity results presented are for a set of 65 ionograms recorded over a 24 hour period between 16/02/05 and 17/02/05. A plot of the maximum number of detected propagating modes for each ionogram is given in Figure 8.10. Maximum capacity for each ionogram was first calculated under the assumption that propagating modes and antennas are fully uncorrelated, by setting mode and antenna correlation matrices to identity matrices of size $m \times m$. The plot of maximum capacity for each ionogram obtained under this assumption is given in Figure 8.11. The average maximum number of propagating modes was 14, while average maximum capacity was 104 bps/Hz.

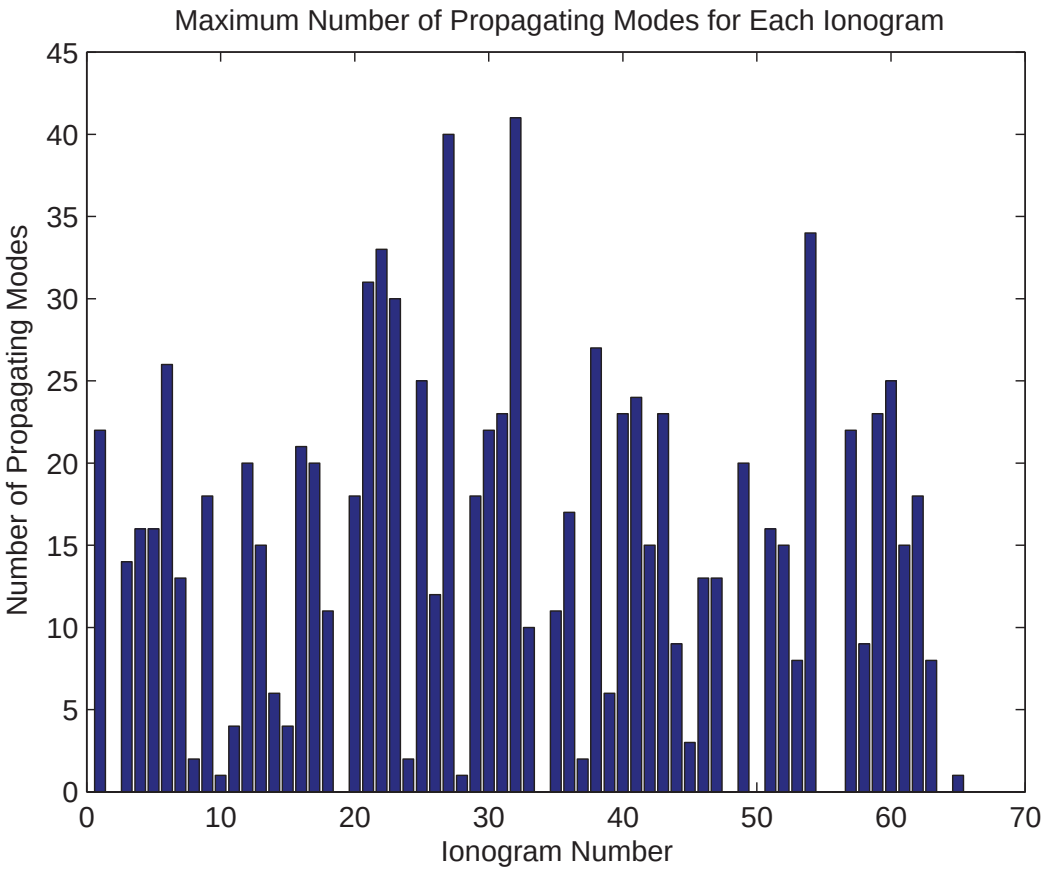

Figure 8.10. Maximum number of propagating modes for each ionogram

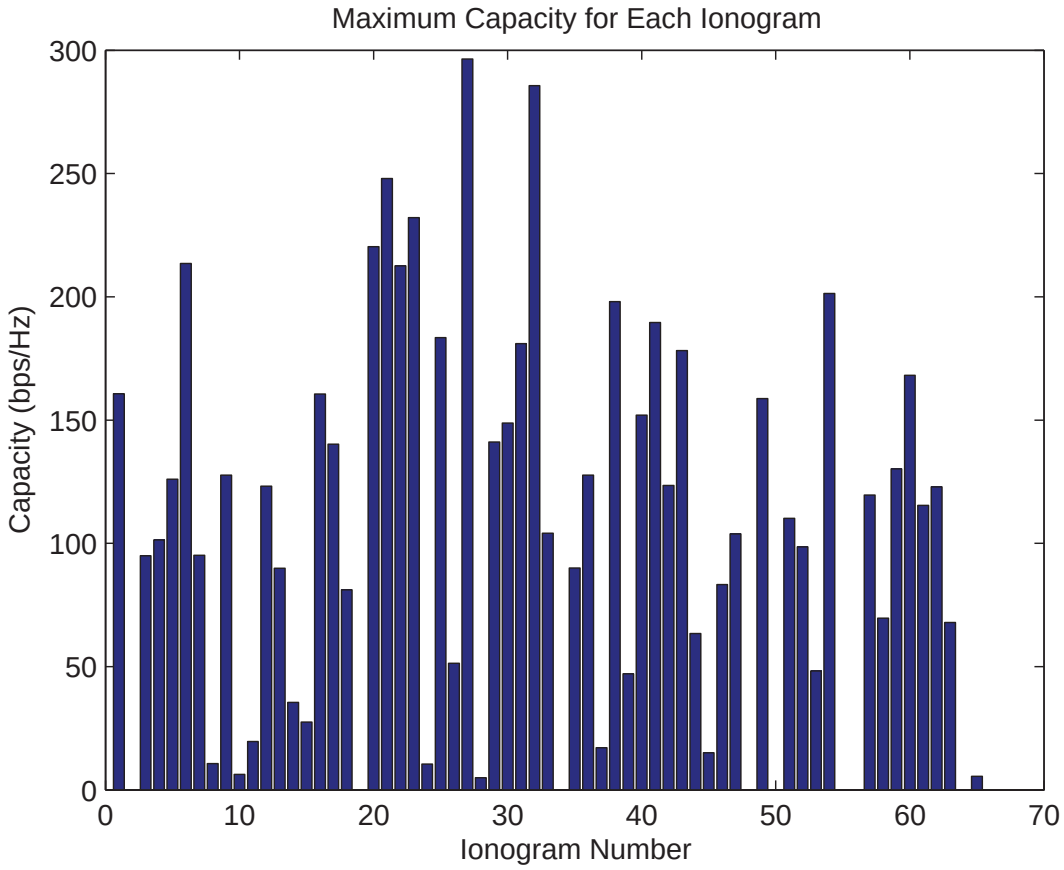

Figure 8.11. Maximum capacity for each ionogram, under the assumption that propagating modes and antennas are fully uncorrelated

Maximum capacity was then recalculated with mode correlation matrices obtained using the technique described in Section 7.2, leaving antenna correlation matrices set to identity matrices of size $m \times m$, so that the underlying capacity of the channel could be investigated. The plot of maximum channel matrix rank for each ionogram is shown in Figure 8.12, while the plot of maximum capacity for each ionogram is given in Figure 8.13. Average maximum channel matrix rank was 10, while average maximum capacity was 94 bps/Hz.

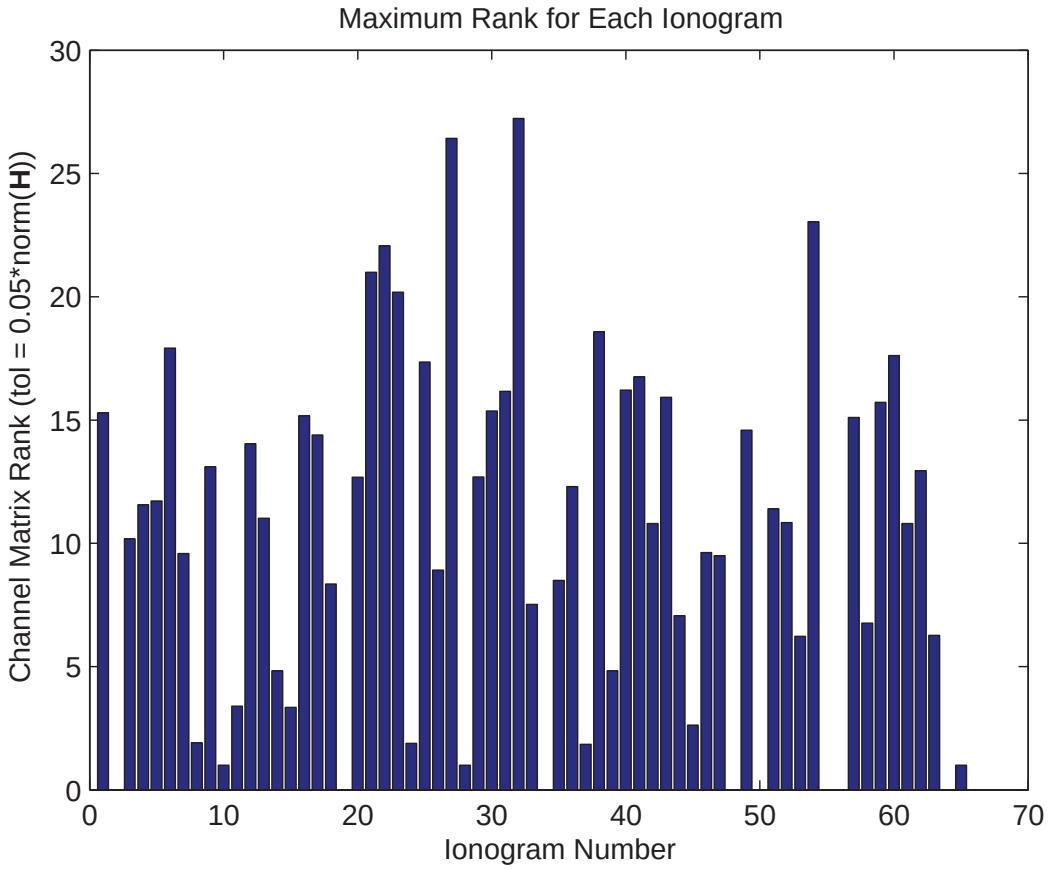

Figure 8.12. Maximum channel matrix rank for each ionogram, taking into account mode correlation under the assumption antennas are fully uncorrelated

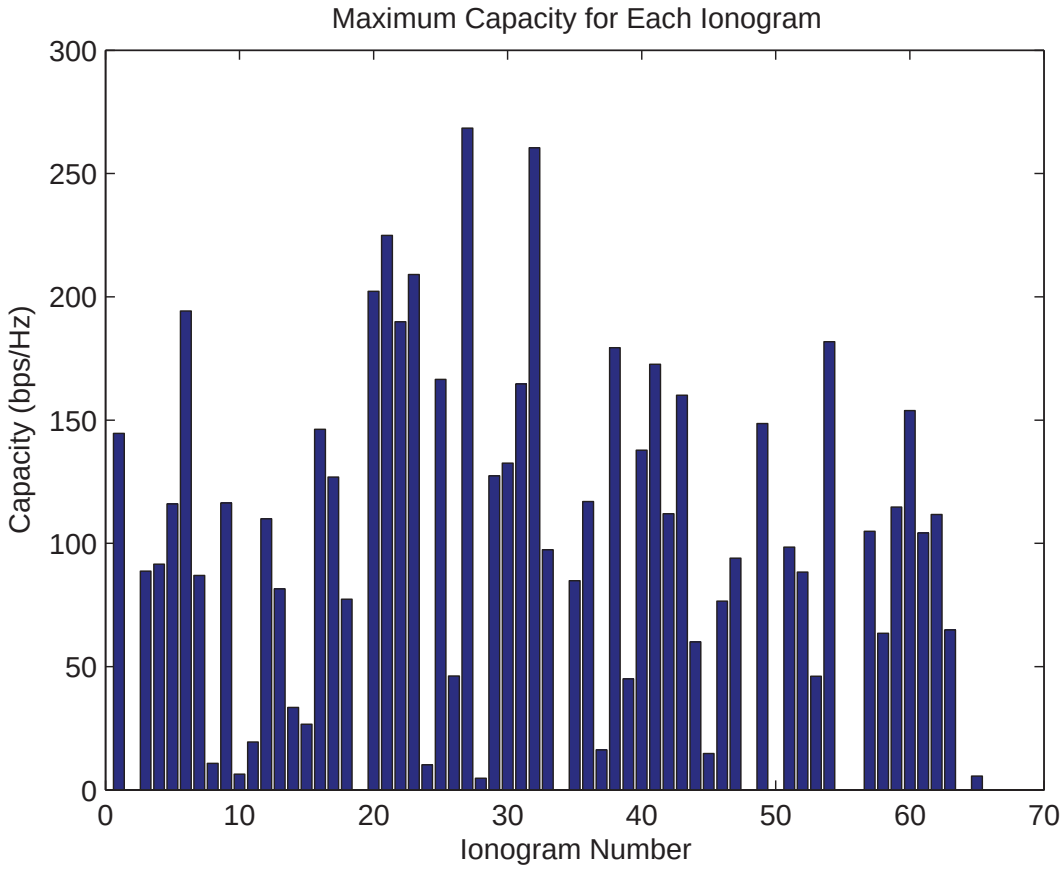

Figure 8.13. Maximum capacity for each ionogram, taking into account mode correlation under the assumption antennas are fully uncorrelated

The maximum capacity calculations were repeated with antenna correlation taken into account by using transmit and receive antenna correlation matrices of size $m \times m$ constructed to represent the average antenna correlation of 0.53 calculated in Section 7.1.1. The plot of maximum channel matrix rank for each ionogram is shown in Figure 8.14, while the plot of maximum capacity for each ionogram is given in Figure 8.15. Average maximum channel matrix rank was 8, while average maximum capacity was 76 bps/Hz.

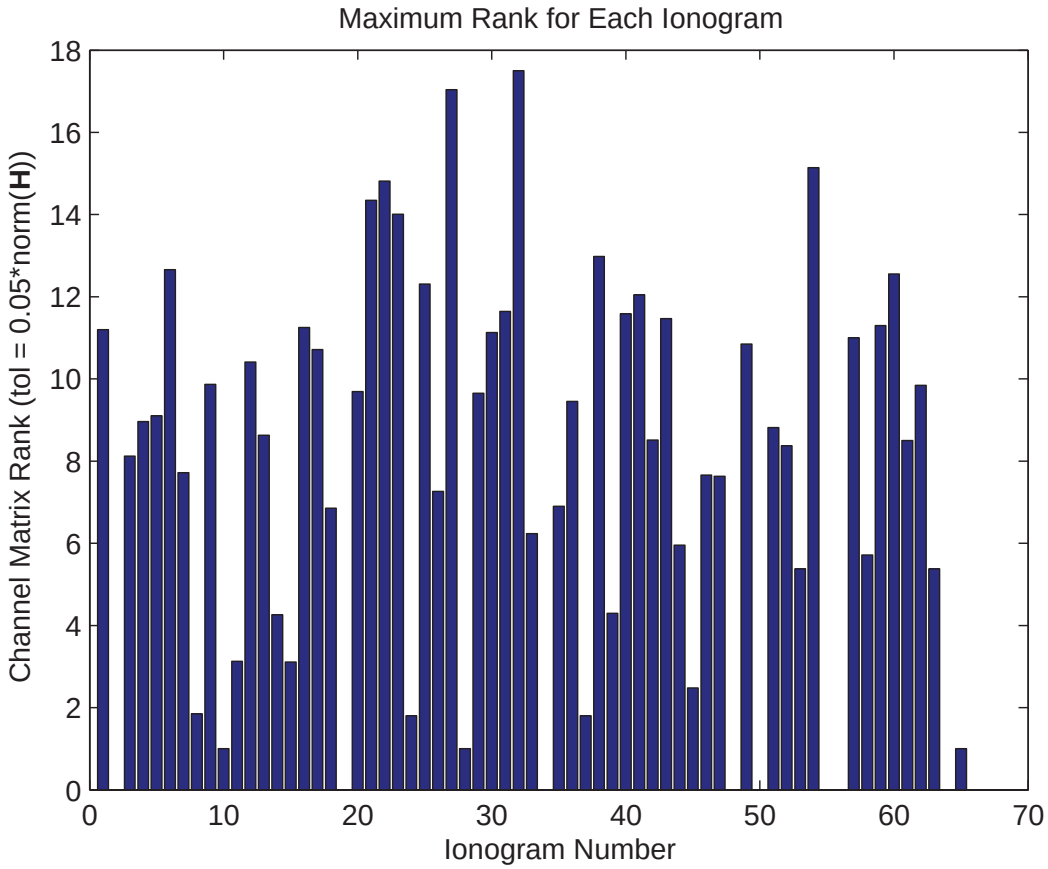

Figure 8.14. Maximum channel matrix rank for each ionogram when both mode and antenna correlation is taken into account

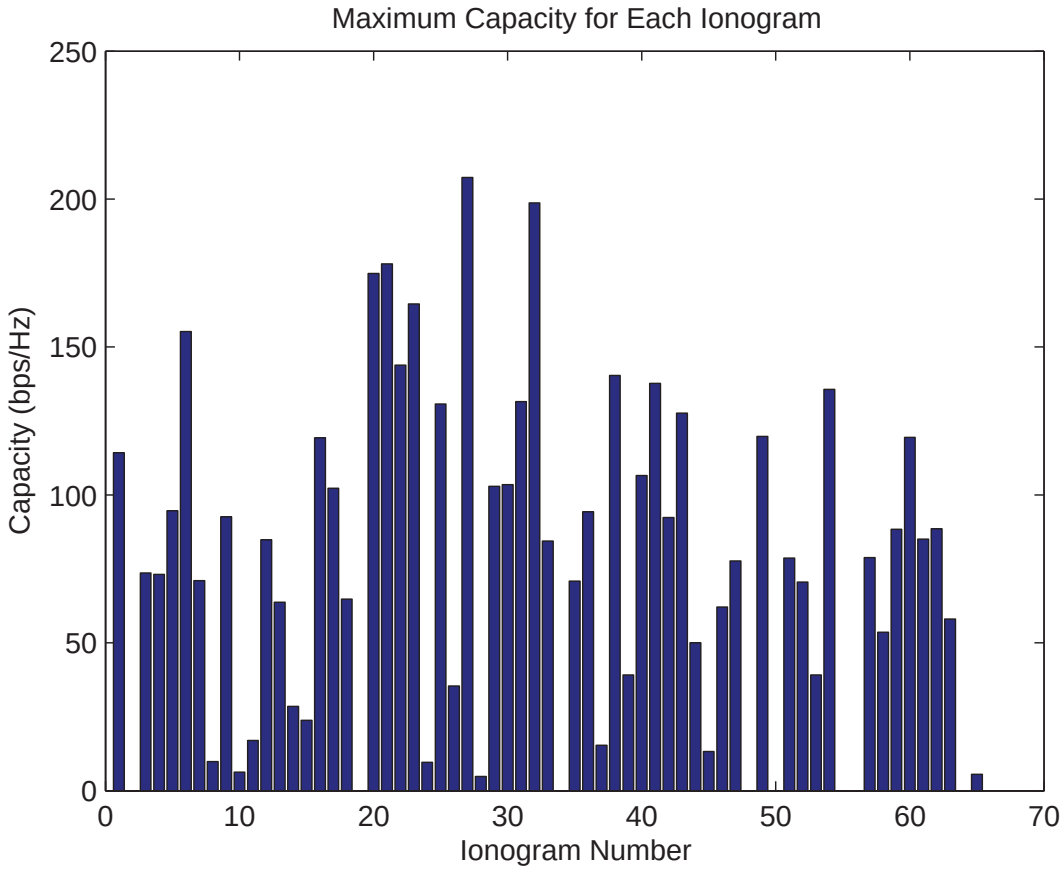

Figure 8.15. Maximum capacity for each ionogram, taking into account both mode and antenna correlation

8.1.3 Accuracy of Capacity Results

The most accurate way to calculate HF MIMO capacity involves building an HF MIMO system, using this system to record channel matrices, and substituting the recorded channel matrices into the general MIMO capacity equation (2.8). The alternative technique devised to calculate HF MIMO capacity in this thesis is a compromise which does not require a full HF MIMO system for data collection, and the results are intended to be used to determine whether developing a full HF MIMO system is worthwhile. Issues concerning the accuracy of the capacity results include spectral resolution, mode correlation calculation, and the Gaussian noise assumption.

Spectral Resolution

The FFT processing which was applied to the HF radio data used a time series data block size of 512 and $N_{FFT} = 2^{20}$. A block size of 512 was used to achieve a good compromise between group delay resolution and ionogram frequency resolution. While FFT resolution is high due to large N_{FFT}, spectral resolution is limited by the small time series data block size used. Limited spectral resolution has an impact on mode and antenna correlation calculations. For mode correlation calculations, consider the situation when two frequencies are closer together than the spectral resolution of the FFT. A single peak is detected at an FFT index in between the FFT indexes of the actual frequencies. Detecting fewer peaks than are actually present leads to a reduced mode correlation matrix rank. For antenna correlation calculations, consider the situation where two frequencies are separated by more than the spectral resolution of the FFT on one antenna, but separated by less than the spectral resolution of the FFT on another antenna. Two distinct frequencies will be detected on the first antenna, while a single frequency will be detected on the second. This situation leads to a reduced antenna correlation value, however antenna correlation calculations are kept conservative by discarding frequency peaks not detected within a small FFT index range on each antenna.

Mode Correlation Calculation

Each consecutive sample of the recorded HF radio data represents both a change in time and a change in frequency. This means that the mode data samples generated for mode correlation calculations are affected by both a change in time and frequency, when only time should change. Mode correlation calculations should be repeated for data collected using a repeating narrowband sweep transmit signal, as described in Chapter 9.

Gaussian Noise Assumption

Gaussian noise is assumed in the derivation of the general MIMO capacity equation (2.8), however the PDF (probability density function) for HF noise is generally not Gaussian [84]. Equation (2.5) of Chapter 2 states that mutual information between the transmit signal vector and the receive signal vector is given by the entropy of receive signal vector minus the entropy of the receive noise vector. The Gaussian distribution is the entropy maximizing distribution, and assuming the receive signal vector distribution to be Gaussian is reasonable, since the transmitter has control over the distribution of the transmit signal vector. Maximizing entropy of the receive signal vector (when receive noise vector entropy is held constant) serves to maximize mutual information, however maximizing entropy of the receive noise vector (when receive signal vector entropy is held constant) serves to minimize mutual information, due to the minus sign in Equation (2.5). The Gaussian noise assumption therefore minimizes capacity and is the most conservative noise distribution assumption that can be made.

8.1.4 Summary of HF MIMO Capacity Results

For the 65 ionograms which were analysed, the average maximum number of detected propagating modes was 14, while the overall maximum number of detected propagating modes exceeded 40. With mode correlation taken into account, average maximum channel matrix rank was 10, and this dropped to 8 when antenna correlation was taken into account. These results suggest that an HF MIMO communication system with 10 uncorrelated transmit and receive antennas will in general capture all of the spatial multiplexing gain available. To counter the reduction in channel matrix rank caused by antenna correlation, either the antenna spacing or the number of antennas used should be increased. Average maximum capacity was 104 bps/Hz

when mode and antenna correlation were neglected, 94 bps/Hz when only mode correlation was taken into account, and 76 bps/Hz when both mode and antenna correlation were taken into account. The capacity with only mode correlation taken into account represents the underlying channel capacity, since the antenna spacing can be increased in order to reduce antenna correlation, however mode correlation cannot be changed. In comparison, for the example ionogram considered in Section 8.1.1, setting $n_T = m = n_R = 1$ reduced maximum average capacity to 9 bps/Hz, which represents the capacity of a single channel HF system in the absence of multipath. The Clover 2000 waveform used in HF modems is designed to operate at a spectral efficiency of 0.25 bps/Hz, however this waveform employs 8 tones in a bandwidth of 2 MHz, so a direct comparison between the MIMO capacities calculated here for the narrow bandwidth of 1.69 Hz, and Clover-2000 spectral efficiency, cannot be made. It can however be concluded from the results that MIMO spatial multiplexing will provide a substantial capacity increase over single channel techniques for the HF channel.

Chapter 9

Conclusion

The HF band is subject to significant multipath caused by multiple refractions and reflections between the ionospheric layers and the earth's surface, making it a possible candidate for spatial multiplexing. In this thesis, the capacity offered by spatial multiplexing in the HF band was investigated. To the best of our knowledge, no such investigation has previously been conducted. The key contributions presented include estimation of HF MIMO capacity from ionograms, development of a multi-channel receiver for HF radio research, development of a model for the HF MIMO channel matrix, and development and application of a technique for estimating HF MIMO capacity from multi-channel receiver data. The results obtained from the investigation indicate that spatial multiplexing offers a significant increase in capacity compared with single channel communication technqiues, and should therefore be seriously considered for future HF radio systems. A major application that stands to benefit from HF MIMO technology is ship based communications. A summary of key results is provided in the following sections, concluding with a description of areas for future research.

9.1 Calculation of HF MIMO Capacity Using Ionosonde Data

In Chapter 4 HF MIMO capacities were calculated using data from the LLISP network of ionosondes under the idealistic assumption that propagating modes are uncorrelated. Most average HF MIMO capacities calculated were found to lie in the range of 40-90 bps/Hz. The promising capacity results obtained, coupled with the issues identified with the LLISP data,

provided motivation for the development of the MCR for HF data collection, and for the continued investigation into HF MIMO capacity.

9.2 HF MIMO Channel Matrix Model

In Chapter 5 a model for the structure of the HF MIMO channel matrix was presented. This model gives an insight into the factors limiting HF MIMO capacity, such as the number of receive antennas n_r, the number of transmit antennas n_t, the number of propagating modes m, and the amount of receive antenna correlation, transmit antenna correlation, and propagating mode correlation present. The following observations can be made about the rank properties of the channel matrix for different antenna and mode correlation conditions when transmit and receive antenna elements are closely spaced

- The presence of either full receive antenna correlation, full transmit antenna correlation, or full mode correlation will yield a rank 1 channel matrix.
- If receive antennas, transmit antennas and modes are fully uncorrelated the channel matrix is full rank, with rank value given by the minimum of n_T, n_R, and m.
- Maximum channel matrix rank is dependent on the number of propagating modes m, and correlation between propagating modes. This is because we have control over the design of the transmit and receive antenna arrays.
- Given m uncorrelated propagating modes we should use m uncorrelated transmit and m uncorrelated receive antennas to achieve the maximum channel matrix rank of m. If some transmit and receive antenna correlation exists, we require $n_T, n_R > m$ to achieve a maximum rank channel matrix.

As transmit and receive antenna element spacing is increased, the structure of the channel matrix becomes more complex, and channel matrix rank increases accordingly. With large antenna element spacing at both the transmit and receive ends, the channel matrix is not limited by the number of propagating modes m, nor the propagating mode correlation. For such a case the channel matrix may be modelled using the Rayleigh channel model.

The rank properties of the channel matrices given by the HF MIMO channel matrix model were found to be the same as the channel matrices given by Gesbert's MIMO channel model.

This finding indicated that HF MIMO capacity could be calculated by measuring antenna and mode correlation matrices, substituting the correlation matrices into Gesbert's MIMO channel model to generate channel matrices, and then substituting the generated channel matrices into the general MIMO capacity equation (2.8) to yield capacity.

9.3 HF MIMO Capacity Calculations

In Chapter 8 HF MIMO capacity calculations were performed on recorded HF radio data by using techniques described in Chapter 7 to generate antenna and mode correlation matrices, substituting these matrices into the Gesbert MIMO channel matrix model equation (5.2) to generate channel matrices, and subsituting the channel matrices into the general MIMO capacity equation (2.8) to yield capacity.

For the 65 ionograms which were analysed, the average maximum number of detected propagating modes was 14, while the overall maximum number of detected propagating modes exceeded 40. With mode correlation taken into account, average maximum channel matrix rank was 10, and this dropped to 8 when antenna correlation was taken into account. These results suggest that an HF MIMO communication system with 10 uncorrelated transmit and receive antennas will in general capture all of the spatial multiplexing gain available. Average maximum capacity was 104 bps/Hz when mode and antenna correlation were neglected, 94 bps/Hz when only mode correlation was taken into account, and 76 bps/Hz when both mode and antenna correlation were taken into account. The capacity with only mode correlation taken into account represents the underlying channel capacity, since the antenna spacing can be increased in order to reduce antenna correlation, however mode correlation cannot be changed. In comparison, for the example ionogram considered in Section 8.1.1, setting $n_T = m = n_R = 1$ reduced maximum average capacity to 9 bps/Hz, which represents the capacity of a single channel HF system in the absence of multipath. The Clover 2000 waveform used in HF modems is designed to operate at a spectral efficiency of 0.25 bps/Hz, however this waveform employs 8 tones in a bandwidth of 2 MHz, so a direct comparison between the MIMO capacities calculated here for the narrow bandwidth of 1.69 Hz, and Clover-2000 spectral efficiency, cannot be made. It can however be concluded from the results that MIMO spatial multiplexing will provide a substantial capacity increase over single channel techniques for the HF channel.

9.4 Possibilities for Future Research

Throughout the course of this thesis a number of areas for future research have been identified, including:

- determining the smallest antenna separation required for adequate antenna decorrelation,
- measuring time correlation of the HF channel, and
- improving mode correlation measurements by using a narrowband sawtooth sweep signal.

The antenna correlation calculations performed in Chapter 7 showed that antenna correlation did not vary noticeably between each pair of antenna elements, so a relationship between antenna separation and antenna correlation, and the minimum antenna separation for adequate decorrelation, could not be determined. These issues can be investigated by repeating antenna correlation calculations with HF radio data collected from a widely spaced linear array of antennas. Determining the minimum antenna separation for adequate decorrelation is important since it indicates the minimum overall array size which does not significantly collapse channel matrix rank.

A technique for calculating the time correlation of the HF channel was described in Section 7.3. In order to perform time correlation calculations, a transmitter which can transmit two FMCW signals of slightly different instantaneous frequency from the same spatial location is required. Time correlation measurements are important since they can be used to determine an appropriate interval between channel matrix estimates which are performed at the receive end of typical MIMO communication systems.

The accuracy of the mode correlation calculations performed in Chapter 7 is limited by the short number of consecutive samples used, and the change in frequency associated with each consecutive sample. If the ionosonde FMCW signal is replaced with a narrowband sawtooth sweep signal, a larger number of consecutive samples can be used in the mode correlation calculations, leading to more accurate results. The narrowband sawtooth sweep signal should be centred on a frequency with a large number of propagating modes. Suitable frequencies can be determined by using a second ionosonde to sweep across the entire HF band.

The use of cross-polarized antennas is another area that should be explored [9], [52], [54].